Theory of dephasing relaxation of excitonic polaritons

T. Takagahara
Department of Applied Physics, The University of Tokyo, Tokyo, 113 Japan
(Received 2 January 1985)

A detailed theory is developed for the dephasing relaxation of the excitonic polariton which was measured recently by Masumoto, Shionoya, and Takagahara [Phys. Rev. Lett. **51**, 923 (1983)] in samples of CuCl crystal by means of nondegenerate four-wave mixing. The concept of dephasing (transverse) relaxation of the excitonic polariton is clarified for the first time and the conceptual difference between the dephasing relaxation of the localized excitation and of the excitonic polariton is emphasized. A method of analysis of the experimental data of the nondegenerate four-wave mixing is presented in detail. The various mechanisms of dephasing relaxation of the excitonic polariton are discussed and examined quantitatively. It is found that the mutual collision among excitonic polaritons is the most probable mechanism that gives the correct order of magnitude of the dephasing relaxation rate and leads to reasonable energy dependence of the relaxation rate in agreement with the experimental results.

I. INTRODUCTION

Recently the dephasing relaxation constant of the excitonic polariton in CuCl was measured by Masumoto, Shionoya, and Takagahara[1] by means of nondegenerate four-wave mixing. The relaxation constant was found to be on the order of 0.01 meV and to increase as the polariton energy approached the exciton resonance from below. Before details are given, it is important to note that there is a conceptual difference between the dephasing relaxation of the localized excitation and of the propagating elementary excitation. In the former case the excitation is localized on an atom or a molecule under consideration. The dephasing relaxation of the localized excitation is related to the decay of the coherence of the relevant optical or nonoptical transition or, in other words, the decay of the off-diagonal component of the density matrix associated with the transition. This dephasing relaxation constant can be directly measured in the time domain by means of time-resolved, degenerate four-wave mixing,[2–5] which is a generalized version of the photon echo.[6] Under irradiation by two light pulses with wave vector and frequency denoted by $(\tilde{k}_1,\omega_1)$ and $(\tilde{k}_2,\omega_1)$, respectively, which are resonant with some material excitation, the intensity of the output pulse with $(2\tilde{k}_2-\tilde{k}_1,\omega_1)$ is measured as a function of the time separation between the two pulses. This measurement is based on the principle that the third-order nonlinear polarization which generates the signal pulse is proportional to the nondephased part of the excitation due to the first pulse at the time when the second delayed pulse reaches the excitation. Thus, the decay of the coherence of the localized excitation can be probed by means of time-resolved, degenerate four-wave mixing.

On the other hand, the proper elementary excitation in solids propagates throughout the crystal with a definite wave vector. Furthermore, it should be noted that the excitonic polariton is a composite particle of exciton and photon. Thus, there arises a conceptual question: What is the dephasing relaxation of the excitonic polariton? The interpretation is not so straightforward as in the case of the localized excitation. The definiteness of the wave vector is one of the salient features of the excitonic polariton which make a remarkable contrast with the case of the localized excitation. The wave vector of the excitonic polariton is primarily determined by the incident light pulse. This wave vector is disturbed by any scattering process, such as impurity scattering, phonon scattering, and polariton-polariton collision. A change of wave vector will lead to the decay of the polarization wave with a definite wave vector. In addition, the electron-hole relative motion of the exciton is also one of the degrees of freedom of the excitonic polariton. The electron-hole relative motion of the exciton may be changed in the scattering processes. This change of the internal degree of freedom leads to the fluctuation and relaxation of the polarization wave, since the oscillator strength of the exciton depends on the exciton internal state. Thus, the concept of dephasing or transverse relaxation of the excitonic polariton is quite different from that of the localized excitation. As a consequence of the definiteness of the wave vector, the wave packet of excitonic polaritons propagates in the crystal with a definite group velocity and there arises an interesting situation from the experimental point of view. The incident photons $(\tilde{k}_1,\omega_1)$ and $(\tilde{k}_2,\omega_1)$ are converted to the excitonic polaritons (k_1,ω_1) and (k_2,ω_1) inside the crystal. The incident photons with the same energy propagate in the crystal with the same group velocity. Thus, in degenerate four-wave mixing, the second delayed polariton pulse (k_2,ω_1) cannot catch up with the first polariton pulse (k_1,ω_1). In order to make the spatial overlap between the two pulses as large as possible, it is essential to make use of nondegenerate four-wave mixing in which the energy of the delayed probe pulse (k_2,ω_2) is suitably chosen so that its group velocity is larger than that of the first pulse (k_1,ω_1). Then the third-order nonlinear polarization will be generated in proportion to the nondephased part of the (k_1,ω_1) pulse and the signal beam with wave

vector and frequency $(2k_2-k_1, 2\omega_2-\omega_1)$ will be emitted. One can obtain information about the dephasing relaxation of the (k_1,ω_1) polariton pulse by measuring the intensity of the output pulse $(2k_2-k_1, 2\omega_2-\omega_1)$ as a function of the relative time delay between the two pulses. To realize the above idea an experiment was carried out for the excitonic polariton in CuCl.[1] It was demonstrated for the first time that the dephasing relaxation of the excitonic polariton could be measured directly in the picosecond time domain by time-resolved, nondegenerate four-wave mixing. The experimental details are given in Ref. 1.

This paper is organized as follows. In Sec. II the propagation dynamics of the excitonic polariton are formulated. The third-order nonlinear polarization in the crystal is calculated perturbationally and the signal intensity of the nondegenerate, four-wave mixing is derived in a suitable form for analysis of the experimental data. In Sec. III experimental data of the correlation trace of nondegenerate four-wave mixing are analyzed to determine the dephasing relaxation constant of the excitonic polariton as a function of energy. In Sec. IV, the various mechanisms of the dephasing (momentum) relaxation of the excitonic polariton are discussed and the relaxation rate due to each mechanism is estimated quantitatively. It is found that mutual collision among excitonic polaritons is the most probable mechanism to cause the dephasing relaxation of the excitonic polariton. In Sec. V, the basic equations of motion for the excitonic polariton are derived quantum mechanically and also the damping constant of the polarization field, which is identified with the dephasing relaxation constant of the excitonic polariton, is derived by the standard statistical mechanical method using the projection operator. Finally in Sec. VI, a few proposals are presented to overcome the difficulty of nondegenerate, four-wave mixing, that the dephasing relaxation constant in the resonance region cannot be determined precisely. In addition a few interesting problems are pointed out for future study.

II. NONDEGENERATE FOUR-WAVE MIXING VIA EXCITONIC POLARITONS

Let us now present the theoretical scheme used to analyze the experimental data. Of main interest is the propagation of excitonic polaritons and their nonlinear interaction in the crystal. Since the excitonic polariton is a composite elementary excitation of exciton and photon, one has to treat the polarization of the material system and the electromagnetic field on an equal footing. The basic equations of motion are given by the constitutive equations for the material polarization due to the exciton and the Maxwell equations for the electromagnetic field. They are written explicitly as

$$\frac{\partial^2}{\partial t^2}P(r,t)+\int_{-\infty}^{\infty}dt'\Gamma(t-t')\frac{\partial}{\partial t'}P(r,t')+\left[\omega_t^2-\frac{\hbar\omega_t}{M}\nabla^2\right]P(r,t)=-\beta\omega_t^2E(r,t)I(r,t)\,, \tag{2.1}$$

$$\frac{\partial}{\partial t}I(r,t)+\gamma_{\|}[I(r,t)-I_0]=\frac{2E(r,t)}{\hbar\omega_t}\left[\frac{\partial}{\partial t}P(r,t)+\tfrac{1}{2}\int_{-\infty}^{\infty}dt'\Gamma(t-t')P(r,t')\right]\,, \tag{2.2}$$

$$\epsilon_\infty\frac{\partial^2}{\partial t^2}E(r,t)-c^2\nabla^2E(r,t)=-4\pi\frac{\partial^2}{\partial t^2}P(r,t)\,, \tag{2.3}$$

with

$$4\pi\beta\omega_t^2/\epsilon_\infty=\omega_l^2-\omega_t^2\,, \tag{2.4}$$

where P, I, and E denote, respectively, the polarization field, the population inversion of the material system, and the electric field; and ω_t (ω_l), M, ϵ_∞, I_0, and $\gamma_{\|}$ are the transverse (longitudinal) exciton frequency, the exciton effective mass, the background dielectric constant, the thermal equilibrium value of I, and the longitudinal (population) relaxation rate, respectively. The damping function $\Gamma(t)$ is related to the dephasing relaxation of the excitonic polariton and its time dependence leads to the frequency-dependent damping constant $\Gamma(\omega)$. Equations (2.1) and (2.2), for the polarization field and the population inversion due to the exciton, are taken from the well-known equations of motion in laser theory[7,8] with modification to include spatial dispersion. In Sec. V, these equations are derived microscopically and their use for the case of excitonic polaritons can be justified. As a matter of course, this set of equations leads to the familiar expression for the dielectric function $\epsilon(k,\omega)$ defined by

$$\epsilon(k,\omega)E(k,\omega)=\epsilon_\infty E(k,\omega)+4\pi P(k,\omega)\,, \tag{2.5}$$

where the spatial and temporal Fourier transforms of the electric and polarization fields are considered. In a situation with no excitation, it is calculated as[9]

$$\epsilon(k,\omega)=\epsilon_\infty+\frac{4\pi\beta\omega_t^2}{\omega_t^2-\omega^2+\hbar\omega_tk^2/M+i\omega\Gamma(\omega)}\,. \tag{2.6}$$

The frequency-dependent or -independent damping constant $\Gamma(\omega)$ is usually introduced phenomenologically. However, as is clear from the above argument, it has the meaning of a damping of the polarization field. In this sense $\Gamma(\omega)$ can be called the dephasing relaxation constant of the excitonic polariton. Our main interest in this paper is how to determine $\Gamma(\omega)$ from the experimental data of nondegenerate four-wave mixing. This is possible because the other material constants ϵ_∞, β, ω_t, and M are determined fairly precisely by hyper-Raman scattering[10,11] and time-of-flight[12,13] measurements.

The spatial distribution of the electric field is shown schematically in Fig. 1 when a monochromatic elec-

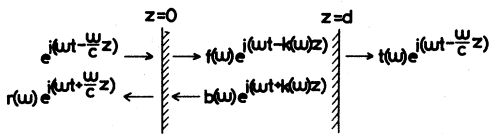

FIG. 1. Schematic representation of the electric field distribution inside and outside a slablike crystal.

tromagnetic field with unit amplitude enters the crystal. The incident laser beam is assumed to propagate normal to the crystal surface. This assumption can be justified because of the small angle of incidence and the large dielectric constant of CuCl. The slablike crystal occupies the region from $z=0$ to $z=d$. The complex wave vector $k(\omega)$ is determined by the dielectric function through the relation

$$\left[\frac{ck}{\omega}\right]^2=\epsilon(k,\omega)\ , \tag{2.7}$$

and is taken to be in the lower half of the complex plane. The coefficients $f(\omega)$ and $b(\omega)$ correspond to the forward- and backward-propagating polariton waves, respectively, and their expressions are obtained from the Maxwell boundary conditions as

$$f(\omega)=\frac{2(\sqrt{\epsilon}+1)}{(\sqrt{\epsilon}+1)^2-(\sqrt{\epsilon}-1)^2e^{-i2k(\omega)d}}\ ,$$
$$b(\omega)=\frac{\sqrt{\epsilon}-1}{\sqrt{\epsilon}+1}e^{-i2k(\omega)d}f(\omega)\ , \tag{2.8}$$

with

$$\sqrt{\epsilon}=ck(\omega)/\omega\ . \tag{2.9}$$

Then the electric field in the crystal is given by

$$[f(\omega)e^{-ik(\omega)z}+b(\omega)e^{ik(\omega)z}]e^{i\omega t}+\text{c.c.} \tag{2.10}$$

These results are obtained for the case of a monochromatic wave. When a pulse or wave packet is considered, the electric field can be decomposed into its Fourier components as

$$\begin{aligned}E_\alpha(t)\cos\omega_\alpha t&=\int_{-\infty}^{\infty}d\omega\, g_\alpha(\omega)e^{i\omega t}(e^{i\omega_\alpha t}+e^{-i\omega_\alpha t})/2\\&=\tfrac{1}{2}\int_{-\infty}^{\infty}d\omega[g_\alpha(\omega+\omega_\alpha)+g_\alpha(\omega-\omega_\alpha)]e^{i\omega t}\\&=\mathrm{Re}\left[\int_0^{\infty}d\omega[g_\alpha(\omega+\omega_\alpha)+g_\alpha(\omega-\omega_\alpha)]e^{i\omega t}\right]=\mathrm{Re}\left[\int_0^{\infty}d\omega\, G_\alpha(\omega)e^{i\omega t}\right],\end{aligned} \tag{2.11}$$

with

$$G_\alpha(\omega)=g_\alpha(\omega+\omega_\alpha)+g_\alpha(\omega-\omega_\alpha)\ , \tag{2.12}$$

where ω_α is the carrier frequency, $E_\alpha(t)$ the pulse envelope, and $g_\alpha(\omega)$ its Fourier transform. The electric field and the polarization field in the crystal can be written as the superposition of monochromatic waves:

$$E(z,t\mid k(\omega_\alpha),\omega_\alpha)=\mathrm{Re}\left[\int_0^{\infty}d\omega\, G_\alpha(\omega)[f(\omega)e^{-ik(\omega)z}+b(\omega)e^{ik(\omega)z}]e^{i\omega t}\right]\ , \tag{2.13}$$

$$P(z,t\mid k(\omega_\alpha),\omega_\alpha)=\mathrm{Re}\left[\int_0^{\infty}d\omega\, G_\alpha(\omega)[\epsilon(k(\omega),\omega)-\epsilon_\infty][f(\omega)e^{-ik(\omega)z}+b(\omega)e^{ik(\omega)z}]e^{i\omega t}/4\pi\right]\ . \tag{2.14}$$

When two light pulses with wave vector and frequency denoted by (k_1,ω_1) and (k_2,ω_2), respectively, enter the crystal, the third-order nonlinear polarization with wave vector $2k_2-k_1$ and frequency $2\omega_2-\omega_1$ will be generated and emit the signal beam to be measured in the experiment. The nonlinear polarization can be calculated perturbationally from the equations of motion (2.1)—(2.3). Starting from the state with no excitation, one has, apart from a proportionality factor,

$$E_\alpha(z,t)=\mathrm{Re}\left[\int_0^{\infty}d\omega\, G_\alpha(\omega)f(\omega)e^{i\omega t-ik(\omega)z}\right]\ , \tag{2.15}$$

$$P_\alpha(z,t)=\mathrm{Re}\left[\int_0^{\infty}d\omega\frac{\beta\omega_t^2G_\alpha(\omega)f(\omega)e^{i\omega t-ik(\omega)z}}{\omega_t^2-\omega^2+\hbar\omega_tk^2(\omega)/M+i\omega\Gamma(\omega)}\right]\ , \tag{2.16}$$

where only the forward-propagating parts in (2.13) and (2.14) are retained and the subscript α $(=1,2)$ indicates the first or second laser pulse. Substituting (2.15) and (2.16) into the right-hand side of (2.2) and extracting the term proportional to $\exp[i(\omega_2-\omega_1)t]$, one obtains

$$\begin{aligned}&\frac{2}{\hbar\omega_t}\int_0^{\infty}d\omega\int_0^{\infty}d\omega'\exp\{i(\omega-\omega')t-i[k(\omega)-k^*(\omega')]z\}G_2(\omega)G_1^*(\omega')f(\omega)f^*(\omega')\\&\quad\times\{[i\omega+\Gamma(\omega)/2]D(\omega,k(\omega))+[-i\omega'+\Gamma(\omega')/2]D^*(\omega',k(\omega'))\}\ ,\end{aligned} \tag{2.17}$$

with

$$D(\omega,k)=\frac{\beta\omega_t^2}{\omega_t^2-\omega^2+\hbar\omega_t k^2/M+i\omega\Gamma(\omega)} . \tag{2.18}$$

The population grating with wave vector k_2-k_1 and frequency $\omega_2-\omega_1$ is calculated from (2.2) as

$$I(k_2-k_1,\omega_2-\omega_1)=\frac{2}{\hbar\omega_t}\int_0^\infty d\omega\int_0^\infty d\omega'\frac{\exp\{i(\omega-\omega')t-i[k(\omega)-k^*(\omega')]z\}}{\gamma_{||}+i(\omega-\omega')}G_2(\omega)G_1^*(\omega')f(\omega)f^*(\omega')$$
$$\times\left[\left[i\omega+\frac{\Gamma(\omega)}{2}\right]D(\omega,k(\omega))+\left[-i\omega'+\frac{\Gamma(\omega')}{2}\right]D^*(\omega',k(\omega'))\right] . \tag{2.19}$$

Then substitution of this population grating into the right-hand side of (2.1) yields the third-order nonlinear polarization $P_{\rm NL}^{(3)}$ with wave vector $2k_2-k_1$ and frequency $2\omega_2-\omega_1$ as

$$P_{\rm NL}^{(3)}(2k_2-k_1,2\omega_2-\omega_1)=-\frac{2}{\hbar\omega_t}\int_0^\infty d\omega\int_0^\infty d\omega'\int_0^\infty d\omega''\frac{\exp\{i(\omega+\omega''-\omega')t-i[k(\omega)+k(\omega'')-k^*(\omega')]z\}}{\gamma_{||}+i(\omega-\omega')}$$
$$\times D(\omega+\omega''-\omega',k(\omega)+k(\omega'')-k^*(\omega'))G_2(\omega)G_2(\omega'')G_1^*(\omega')$$
$$\times f(\omega)f(\omega'')f^*(\omega')\left[\left[i\omega+\frac{\Gamma(\omega)}{2}\right]D(\omega,k(\omega))\right.$$
$$\left.+\left[-i\omega'+\frac{\Gamma(\omega')}{2}\right]D^*(\omega',k(\omega'))\right] . \tag{2.20}$$

This nonlinear polarization will generate a signal electric field, acting as the source term on the right-hand side of (2.3), which is given by

$$E(2k_2-k_1,2\omega_2-\omega_1)=-\frac{2}{\hbar\omega_t}\int_0^\infty d\omega\int_0^\infty d\omega'\int_0^\infty d\omega''\frac{4\pi(\omega+\omega''-\omega')^2F(\omega,\omega',\omega'')}{-\epsilon_\infty(\omega+\omega''-\omega')^2+c^2[k(\omega)+k(\omega'')-k^*(\omega')]^2} , \tag{2.21}$$

where $F(\omega,\omega',\omega'')$ denotes the whole integrand on the right-hand side of (2.20). This electric field is the field within the slablike crystal but not the signal field to be observed outside the crystal. The latter has to be calculated from the Maxwell equations and the associated boundary conditions.

Within the nonlinear crystal, the homogeneous electric fields are usually associated with the nonlinearly induced electric field whose wave vector is not necessarily identical to that of the homogeneous wave. These homogeneous fields arise as a due consequence of the Maxwell boundary conditions.[14] In Fig. 2 the configuration of the nonlinearly induced wave and the associated homogeneous waves is shown schematically, where the electric field corresponding to the backward-propagating nonlinear polarization is neglected owing to its smallness. Assuming the normal incidence of the laser beams the electric field for each wave in Fig. 2 can be written as

$$E_s e^{i(\omega t-K_s z)},\quad E_r e^{i(\omega t+K_0 z)},\quad E_t e^{i\omega t-iK_0(z-d)},$$
$$E_f e^{i(\omega t-K_h z)},\quad E_b e^{i(\omega t+K_h z)}, \tag{2.22}$$

with $\omega=2\omega_2-\omega_1$, $K_s=2k(\omega_2)-k^*(\omega_1)$, $K_0=\omega/c$, and $K_h=k(\omega)$, where E_s, E_r, and E_t correspond to the nonlinearly induced field, the reflected field, and the electric field to be observed outside the crystal, respectively, and E_f and E_b correspond to the associated homogeneous waves. From the Maxwell boundary conditions at $z=0$ and $z=d$, the four relations among E_s, E_r, E_t, E_f, and E_b are obtained:

$$E_s+E_f+E_b=E_r,\quad n_sE_s+n(E_f-E_b)=-E_r ,$$
$$E_s e^{-iK_s d}+E_f e^{-iK_h d}+E_b e^{iK_h d}=E_t , \tag{2.23}$$
$$n_sE_s e^{-iK_s d}+n(E_f e^{-iK_h d}-E_b e^{iK_h d})=E_t ,$$

where n_s and n are defined by

$$n_s=cK_s/\omega,\quad n=cK_h/\omega . \tag{2.24}$$

The amplitude E_t is calculated as

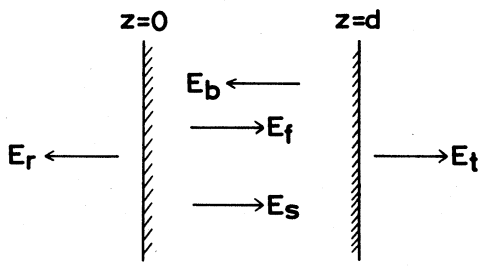

FIG. 2. Schematic representation of electric field amplitudes with frequency $2\omega_2-\omega_1$. E_s, E_r, and E_t represent the nonlinearly induced wave, the reflected wave, and the transmitted wave, respectively, and E_f and E_b are the forward- and backward-propagating homogeneous waves.

$$\frac{E_t}{E_s}=\frac{(1-n)(n-n_s)(e^{-i(K_s+K_h)d}-1)+(1+n)(n+n_s)(e^{-i(K_s-K_h)d}-1)}{(1+n)^2e^{iK_hd}-(1-n)^2e^{-iK_hd}} \tag{2.25}$$

or can be rewritten as

$$\frac{E_t}{E_s}=\frac{i(n^2-n_s^2)\omega/c}{(1+n)^2e^{iK_hd}-(1-n)^2e^{-iK_hd}}\int_0^d dz[(n+1)e^{-i(K_s-K_h)z}+(n-1)e^{-i(K_s+K_h)z}] . \tag{2.26}$$

Combining all the results, the expression of the electric field amplitude to be measured outside the crystal is given by

$$\begin{aligned}E_{\rm obs}(R,t)=-\frac{2i}{c\hbar\omega_t}\int_0^d dz\int_0^\infty d\omega\int_0^\infty d\omega'\int_0^\infty d\omega''&\left[\frac{\omega_s(n^2-n_s^2)}{(1+n)^2e^{iK_hd}-(1-n)^2e^{-iK_hd}}\right]\\ &\times\left[\frac{4\pi\omega_s^2}{[\gamma_{\|}+i(\omega-\omega')](c^2K_s^2-\epsilon_\infty\omega_s^2)}\right]G_2(\omega)G_1^*(\omega')\\ &\times G_2(\omega'')f(\omega)f^*(\omega')f(\omega'')D(\omega_s,K_s)\\ &\times\left[\left[i\omega+\frac{\Gamma(\omega)}{2}\right]D(\omega,k(\omega))+\left[-i\omega'+\frac{\Gamma(\omega')}{2}\right]D^*(\omega',k(\omega'))\right]\\ &\times[(n+1)e^{-i(K_s-K_h)z}+(n-1)e^{-i(K_s+K_h)z}]\exp\left[i\omega_s\left[t-\frac{R-d}{c}\right]\right],\end{aligned} \tag{2.27}$$

with

$$\omega_s=\omega+\omega''-\omega',\quad K_s=k(\omega)+k(\omega'')-k^*(\omega') ,$$
$$K_h=k(\omega_s),\quad n_s=cK_s/\omega_s ,\quad n=cK_h/\omega_s , \tag{2.28}$$

where R is the z coordinate of the observation point. This expression is quite general but contains a fourfold integral, which is a rather heavy task to perform straightforwardly. It is desirable to simplify the expression by introducing reasonable approximations. The integrations with respect to ω, ω', and ω'' are over the spectral width of the incident laser pulses. If a function contained in the integrand is slowly varying over the region where the spectral function $G_\alpha(\omega)$ takes significant values, it can be put outside the integral and replaced by its value at the peak position of $G_\alpha(\omega)$. In this spirit of simplification, all of the factors within the integrand on the right-hand side of (2.27) can be put outside the integral except for the exponential factors. This simplification can be justified under the condition that

$$\omega_1,\omega_2\gg\Delta\omega,\quad \Delta\omega/v_g(\omega)k(\omega)\ll 1 , \tag{2.29}$$

where $\Delta\omega$ denotes the typical spectral width of the incident laser pulses, and v_g is the group velocity of the excitonic polariton. Then the expression (2.27) can be greatly simplified to

$$\begin{aligned}E_{\rm obs}(R,t)\propto\int_0^d dz\int_0^\infty d\omega\int_0^\infty d\omega'\int_0^\infty d\omega''&G_2(\omega)G_2(\omega'')G_1^*(\omega')\exp\left[i(\omega+\omega''-\omega')\left[t-\frac{R-d}{c}\right]\right]\\ &\times[(\bar n+1)e^{-i(K_s-K_h)z}+(\bar n-1)e^{-i(K_s+K_h)z}] ,\end{aligned} \tag{2.30}$$

with

$$\bar n=ck(2\omega_2-\omega_1)/(2\omega_2-\omega_1) ,$$

where the unimportant multiplicative factors are omitted. At this stage the threefold frequency integral is reduced to a separable form and can be performed easily. The ω dependence of $k(\omega)$ in the exponent is expanded up to the first-order term as

$$k(\omega)=k(\bar\omega)+\frac{dk}{d\omega}(\omega-\bar\omega)+\ldots=k(\bar\omega)+\frac{\omega-\bar\omega}{v_g(\bar\omega)}+\ldots , \tag{2.31}$$

where $\bar\omega$ denotes the peak position of a spectral function $G(\omega)$. Then the threefold frequency integral in (2.30) can be simplified as

$$E_{\rm obs}(R,t)\propto \exp[i(2\omega_2-\omega_1)t_R]$$
$$\times\int_0^d dz\int_0^\infty d\omega\int_0^\infty d\omega'\int_0^\infty d\omega'' G_2(\omega)G_1^*(\omega')G_2(\omega'')\exp\{-i[2k(\omega_2)-k^*(\omega_1)]z+i(\Delta+\Delta''-\Delta')t_R\}$$
$$\times\{(\bar n+1)\exp[ik_h z-i(1/v_2-1/v_h)(\Delta+\Delta'')z+i(1/v_1-1/v_h)\Delta' z]$$
$$+(\bar n-1)\exp[-ik_h z-i(1/v_2+1/v_h)(\Delta+\Delta'')z+i(1/v_1+1/v_h)\Delta' z]\}\ , \tag{2.32}$$

with the abbreviations:

$$\Delta=\omega-\omega_2,\ \ \Delta'=\omega'-\omega_1,\ \ \Delta''=\omega''-\omega_2,\ \ v_1=v_g(\omega_1),\ \ v_2=v_g(\omega_2)\ ,$$
$$v_h=v_g(2\omega_2-\omega_1),\ \ k_h=k(2\omega_2-\omega_1),\ \ \bar n=ck_h/(2\omega_2-\omega_1),\ \ t_R=t-\frac{R-d}{c}\ . \tag{2.33}$$

Making use of the relation

$$\int_0^\infty d\omega\, G_\alpha(\omega)e^{i\Delta t}=\int_0^\infty d\omega[g_\alpha(\omega+\omega_\alpha)+g_\alpha(\omega-\omega_\alpha)]e^{i(\omega-\omega_\alpha)t}\cong\int_{-\infty}^\infty d\omega\, g_\alpha(\omega-\omega_\alpha)e^{i(\omega-\omega_\alpha)t}=E_\alpha(t)\ , \tag{2.34}$$

one can further simplify (2.32) to

$$E_{\rm obs}(R,t)\propto\int_0^d dz\exp\{-i[2k(\omega_2)-k^*(\omega_1)]z\}$$
$$\times\{(\bar n+1)e^{ik_h z}[E_2(t_R+(1/v_h-1/v_2)z)]^2E_1(t_R+(1/v_h-1/v_1)z)$$
$$+(\bar n-1)e^{-ik_h z}[E_2(t_R-(1/v_h+1/v_2)z)]^2E_1(t_R-(1/v_h+1/v_1)z)\}\ . \tag{2.35}$$

The second term in the second pair of curly brackets of (2.35) contains a factor which is rapidly oscillating with respect to z and gives a smaller contribution to $E_{\rm obs}$ than the first term. In the following only the first term will be considered. The physical quantity observed in the experiment is the integrated intensity of the signal field, namely,

$$\int_{-\infty}^\infty dt\,|E_{\rm obs}(t)|^2\ . \tag{2.36}$$

The correlation trace is obtained by repeating the same measurement while changing the delay time τ_d of the second pulse relative to the first pulse. When the shapes of the two pulses are identical, the signal field is given by

$$E_{\rm obs}(R,t)\propto\int_0^d dz\exp\{i[k_h-2k(\omega_2)+k^*(\omega_1)]z\}[E(t_R+(1/v_h-1/v_2)z)]^2E(t_R+\tau_d+(1/v_h-1/v_1)z)\ , \tag{2.37}$$

where $E(t)$ is the common pulse envelope. The expression is remarkably simple and important in the analysis of the experimental data.

It is instructive to look into the limiting form of the correlation trace when all the incident pulses are δ-function-like. In this case the signal field is calculated as

$$E_{\rm obs}(R,t)\propto\int_0^d dz\,e^{i\Delta kz}[\delta(t_R+(1/v_h-1/v_2)z)]^2\delta(t_R+\tau_d+(1/v_h-1/v_1)z)$$
$$=\int_0^d dz\,e^{i\Delta kz}[\delta(t_R+(1/v_h-1/v_2)z)]^2\delta(\tau_d+(1/v_2-1/v_1)z)$$
$$\propto\Theta(\tau_d)\Theta(d(1/v_1-1/v_2)-\tau_d)[\delta(t_R+(1/v_h-1/v_2)\tau_d/(1/v_1-1/v_2))]^2\exp[i\Delta k\tau_d/(1/v_1-1/v_2)]\ , \tag{2.38}$$

with

$$\Delta k=k_h-2k(\omega_2)+k^*(\omega_1)\ ,$$

where Θ is the Heaviside step function and the inequality $v_1<v_2$ is implicitly assumed because $\omega_2<\omega_1<\omega_l$ in the experiment. The integrated intensity of the signal field becomes

$$\int_{-\infty}^\infty dt\,|E_{\rm obs}(t)|^2\propto\Theta(\tau_d)\Theta(d(1/v_1-1/v_2)-\tau_d)\exp\{-2[2k_i(\omega_2)+k_i(\omega_1)-k_i(2\omega_2-\omega_1)]\tau_d/(1/v_1-1/v_2)\}\ , \tag{2.39}$$

where $k_i(\omega)$ is the imaginary part of the wave vector defined by

$$k(\omega)=k_r(\omega)-ik_i(\omega),\ \ k_i(\omega)>0\ . \tag{2.40}$$

Thus, the correlation trace is nonzero only within the range from $\tau_d=0$ to $\tau_d=d(1/v_1-1/v_2)$ and shows a quite asymmetric form as depicted in Fig. 3. In this ideal limit, one can estimate $2k_i(\omega_2)+k_i(\omega_1)-k_i(2\omega_2-\omega_1)$ from the decay rate of the correlation trace. Furthermore, by varying ω_1 and ω_2 appropriately, one can determine $k_i(\omega)$ at each ω and accordingly $\Gamma(\omega)$ in principle. The decay rate in (2.39) has a clear physical meaning. The length $\tau_d/(1/v_1-1/v_2)$ is nothing but the depth in the crystal where the two δ-function-like pulses meet and the nonlinear interaction occurs. Before the two pulses overlap spatially, each polariton wave suffers spatial damping

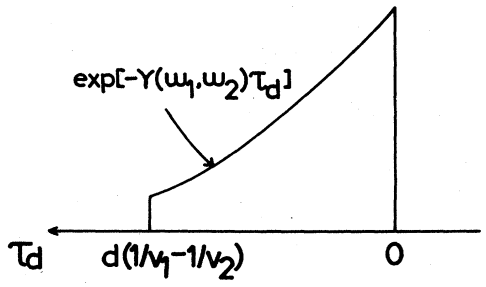

FIG. 3. A typical correlation trace of nondegenerate four-wave mixing under a limiting situation in which the two incident pulses are δ-function-like. $\gamma(\omega_1,\omega_2)$ is given by $2[2k_i(\omega_2)+k_i(\omega_1)-k_i(2\omega_2-\omega_1)]/(1/v_1-1/v_2)$.

due to the imaginary part k_i of the wave vector. The generated nonlinear polarization emits the electromagnetic field, which is observed as a signal field outside the crystal. This signal field with frequency $2\omega_2-\omega_1$ propagates in the crystal as a polariton wave and suffers spatial damping during the passage from $z=\tau_d/(1/v_1-1/v_2)$ to $z=d$, i.e., the rear surface of the sample. These spatial dampings lead to the decay rate in (2.39).

III. ANALYSIS OF EXPERIMENTAL DATA

In this section the experimental data of the correlation trace are analyzed on the basis of the general theory developed in Sec. II and the dephasing relaxation constant $\Gamma(\omega)$ of the excitonic polariton is determined as a function of energy. The electric field at the observation point is given by (2.37) and the integrated signal intensity is calculated as

$$\begin{aligned} I(\tau_d)&=\int_{-\infty}^{\infty}dt\,|E_{\rm obs}(R,t)|^2 \\ &=\int_{-\infty}^{\infty}dt\int_0^d dz\int_0^d dz' e^{iKz-iK^*z'}E^2(t+\alpha z) \\ &\quad\times E(t+\tau_d+\beta z)E^2(t+\alpha z') \\ &\quad\times E(t+\tau_d+\beta z') \end{aligned} \tag{3.1}$$

with

$$\begin{aligned} &K=k(2\omega_2-\omega_1)-2k(\omega_2)+k^*(\omega_1)=K_r+iK_i\ , \\ &\alpha=1/v_h-1/v_2,\quad \beta=1/v_h-1/v_1\ , \end{aligned} \tag{3.2}$$

where the real and imaginary parts of K are denoted by K_r and K_i, respectively. In the following the incident pulse envelope $E(t)$ is supposed to be Gaussian:

$$E(t)\propto\exp(-t^2/2\sigma^2)\ , \tag{3.3}$$

where σ characterizes the pulse width. Calculating the time integral in (3.1) first, and changing the integration variables z and z' to x and y defined by $x=z+z'$ and $y=z-z'$, one obtains

$$\begin{aligned} I(\tau_d)&=\frac{\sigma}{2}\left[\frac{\pi}{3}\right]^{1/2}\left[\int_0^d dx\int_{-x}^{x}dy+\int_d^{2d}dx\int_{x-2d}^{2d-x}dy\right]\exp\left[-\frac{[(\alpha-\beta)x-2\tau_d]^2}{6\sigma^2}-K_ix-D\left[y-\frac{iK_r}{2D}\right]^2-\frac{K_r^2}{4D}\right] \\ &=\left[\frac{\pi\sigma^2}{3D}\right]^{1/2}\exp\left[-\frac{(K_r)^2}{4D}\right]{\rm Re}\left\{\int_0^d dx\exp\left[-\frac{[(\alpha-\beta)x-2\tau_d]^2}{6\sigma^2}-K_ix\right]{\rm erf}\left[\sqrt{D}\left[x-\frac{iK_r}{2D}\right]\right]\right. \\ &\quad\left.+\int_d^{2d}dx\exp\left[-\frac{[(\alpha-\beta)x-2\tau_d]^2}{6\sigma^2}-K_ix\right]{\rm erf}\left[\sqrt{D}\left[2d-x-\frac{iK_r}{2D}\right]\right]\right\} \end{aligned} \tag{3.4}$$

with

$$D=(2\alpha^2+\beta^2)/4\sigma^2\ , \tag{3.5}$$

where the error function with complex argument z is defined by

$${\rm erf}[z]=\int_0^z dt\exp(-t^2)\ , \tag{3.6}$$

and its real part is given by

$${\rm Re\,erf}[z=x+iy]={\rm erf}[x]+e^{-x^2}\int_0^{|y|}dt\,e^{t^2}\sin 2xt\ . \tag{3.7}$$

It is now instructive to examine the case where the two incident pulses have the same energy, i.e., $\omega_1=\omega_2$. In this case the denominator $\gamma_{||}+i(\omega-\omega')$ in (2.27) cannot be simply put outside the integral because $\omega-\omega'$ can become zero. Employing the Gaussian pulse envelope (3.3) and carrying out the frequency integral in (2.27), one obtains

$$E_{\rm obs}(R,t)\propto\int_0^d dz\exp[-2k_i(\omega_1)z]\int_{-\infty}^{\infty}dx\frac{\exp[-\sigma^2x^2/4+ix(t_R+\tau_d/2)]}{\gamma_{||}+ix}\ , \tag{3.8}$$

where $t_R = t - (R-d)/c$ and k_i is defined by (2.40). The important point to be noted is that τ_d and $k_i(\omega)$ are contained in a separate manner. Thus, $k_i(\omega)$ or equivalently $\Gamma(\omega)$ cannot be determined from the correlation trace, i.e., from the τ_d dependence of the integrated signal intensity. This confirms the importance of nondegenerate four-wave mixing in the study of the dephasing relaxation of the excitonic polariton as mentioned in the Introduction.

In the experiment the energy of the second pulse ω_2 is fixed at the transparent region of the crystal, while that of the first pulse ω_1 is varied over the resonance region as shown in Fig. 4. The energy of the nonlinearly mixed light $2\omega_2-\omega_1$ lies in the far off-resonance region. As seen from (3.2), the imaginary part K_i is dependent on $\Gamma(\omega)$ at three energy points, namely, $\Gamma(\omega_1)$, $\Gamma(\omega_2)$, and $\Gamma(2\omega_2-\omega_1)$. The one of most interest is $\Gamma(\omega_1)$, since the others are values in the off-resonance region. The values of $\Gamma(\omega_2)$ and $\Gamma(2\omega_2-\omega_1)$ are taken from the data of reflectivity and transmission measurements.[15] The value of $\Gamma(\omega_1)$ is left as an adjustable parameter for the curve fitting. In the numerical calculation of the correlation trace, the dispersion relation of the excitonic polariton in CuCl is used; the dispersion relation has been studied recently in detail.[10–13,16] The parameter σ is determined from the experimental pulse width (full width at half maximum or FWHM) of 20 ps. The theoretical results are indicated by closed circles in Fig. 5. The spatial overlap between the two pulses and accordingly the integrated signal intensity become larger, in the case of a later arrival of the second pulse, than in the case of an earlier arrival, since the group velocity of the second pulse is quite large. The extreme case of this feature is demonstrated in Fig. 3 for δ-function-like pulses. In reality, the incident pulse has a finite width and the correlation trace in Fig. 3 becomes broadened. The asymmetry of the correlation trace in Fig. 5 can be understood in this way. The values of Γ determined from the curve fitting are given in Fig. 6. The right-hand ordinate indicates the dephasing relaxation

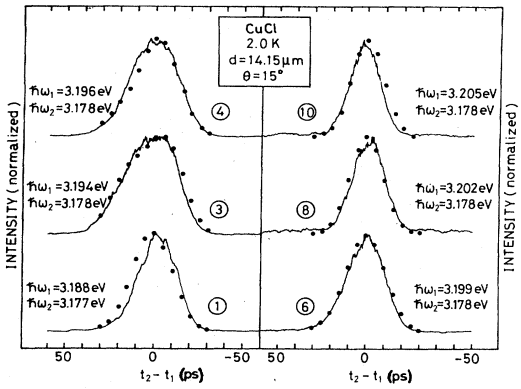

FIG. 5. Integrated intensity of the $2\omega_2-\omega_1$ beam emitted from a 14.15-μm-thick CuCl crystal as a function of the relative time delay $\tau_d = t_2 - t_1$ between ω_2 and ω_1 pulses.

time $\hbar/(\Gamma/2)$ of the excitonic polariton. As seen in Fig. 6, Γ is of the order of 0.01 meV independent of the sample thickness and increases as the energy approaches the exciton resonance. When the energy ω_1 approaches the exciton resonance, the correlation trace becomes nearly symmetric with respect to $\tau_d = 0$ and insensitive to the change of ω_1. This feature can be understood on the basis of (3.4). In the resonance region the group velocity of the excitonic polariton is quite small and one can employ the following approximations:

$$\alpha - \beta \cong 1/v_1, \quad D \cong (4\sigma^2 v_1^2)^{-1} . \tag{3.9}$$

Since the ratio v_1/c is typically 10^{-4}, the Gaussian factor

$$\exp\{-[(\alpha-\beta)x - 2\tau_d]^2/6\sigma^2\}$$

in (3.4) represents a very sharp distribution whose peak position and width are both of the order of 1 μm or less. Thus, when the sample thickness d is about 20–30 mic-

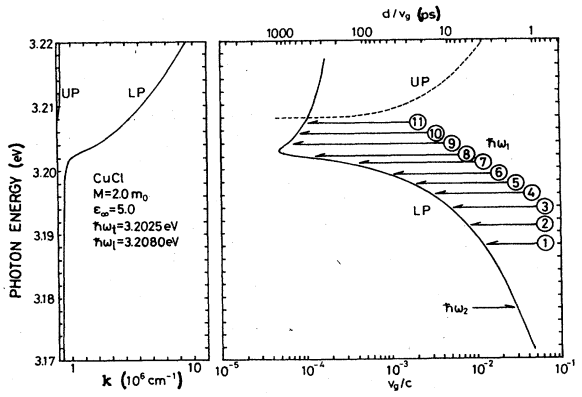

FIG. 4. Left: Dispersion relation of the excitonic polariton in CuCl, shown for both the upper- (UP) and lower- (LP) branch polaritons. Right: Group velocity of the excitonic polariton normalized by light velocity c in vacuum (lower abscissa) and the calculated transit time of the polariton pulse through a 14.15-μm-thick CuCl crystal (upper abscissa). The energy $\hbar\omega_1$ is varied from 1 to 11, whereas $\hbar\omega_2$ is fixed at the transparent region.

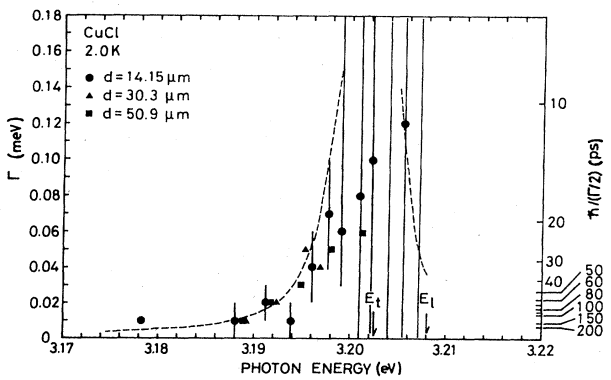

FIG. 6. Dephasing relaxation constant Γ as a function of energy of the excitonic polariton in CuCl. The three data symbols correspond to samples of different thicknesses. Long error bars above 3.200 eV mean that Γ cannot be determined precisely. The dashed line is the calculated energy dependence of Γ based on a model of polariton-polariton scattering (see text).

rons, the second integral in (3.4) can be neglected and one finds for positive τ_d

$$I(\tau_d) \propto \exp\left[-\frac{K_r^2}{4D}-\frac{2K_i\tau_d}{\alpha-\beta}\right] \times \mathrm{Re\,erf}\left[\sqrt{D}\left[\frac{2\tau_d}{\alpha-\beta}-\frac{iK_r}{2D}\right]\right] . \tag{3.10}$$

Substitution of (3.9) into (3.10) leads to

$$I(\tau_d) \propto \exp[-(v_1\sigma K_r)^2-2v_1K_i\tau_d]\,\mathrm{Re\,erf}[\tau_d/\sigma-iv_1\sigma K_r] . \tag{3.11}$$

Since $v_1\sigma K_r$ is large and typically of the order of 10^2, one can use an approximate formula derived from (3.7) for $y \gg 1$:

$$e^{-y^2}\mathrm{Re\,erf}[x+iy] \cong e^{-x^2}\int_0^{|y|} dt\, \exp(t^2-y^2)\sin 2xt . \tag{3.12}$$

Because the integral factor in (3.12) has only a weak dependence on x, the characteristic dependence of the correlation trace on τ_d is given by

$$I(\tau_d) \propto \exp[-2v_1K_i\tau_d-(\tau_d/\sigma)^2] . \tag{3.13}$$

For a typical value of K_i of about 10^4 cm^{-1} and for σ of the order of 10 ps, the τ_d dependence of the correlation trace is dominated by the second exponent in (3.13) and the profile becomes insensitive to the change of ω_1 in the exciton resonance region. Thus, the value of K_i or equivalently $\Gamma(\omega)$ cannot be determined precisely in the resonance region. However, even in a situation where the correlation trace is limited by the incident pulse width, the upper limit of $\Gamma(\omega)$ can be estimated from the relation

$$2v_1K_i < \sigma^{-1} . \tag{3.14}$$

IV. MECHANISMS OF DEPHASING RELAXATION OF EXCITONIC POLARITONS

Let us now discuss the mechanism of the dephasing relaxation of excitonic polaritons. As mentioned in the Introduction, the relaxation to be observed in the experiment depends in general on the method of measurement. In the four-wave mixing experiment not only the incident laser beams but also the generated signal beam are spatially well collimated. Thus, any mechanism which causes a momentum change of the excitonic polariton will lead to the decay of the macroscopic polarization with a well-defined wave vector. Even elastic scattering leads to the decay of the polarization field, namely, the dephasing relaxation of the excitonic polariton in the case of four-wave mixing. This is in striking contrast to the case of induced absorption (IA).[17–19] In the case of IA all the polaritons that are scattered elastically into various directions can contribute to the absorption signal since only the energy is relevant in the absorption process and the direction of the polariton wave vector does not matter. The decay-time constant of IA reflects the energy relaxation of the ensemble of the injected polaritons. On the other hand, momentum relaxation by some mechanisms contributes to the dephasing relaxation of excitonic polaritons. The most likely mechanisms to cause such dephasing or momentum relaxation are (a) impurity scattering, (b) phonon scattering, and (c) polariton-polariton scattering.

Assuming the impurity-polariton scattering matrix element M to be independent of the momentum transfer, one can calculate the momentum relaxation rate due to the impurity scattering as

$$\Gamma_{\mathrm{imp}}(k)=\frac{2\pi}{\hbar}|M|^2\sum_q \delta(E(k+q)-E(k))=\frac{|M|^2V}{2\pi\hbar}\int_0^{2k} dq\, q^2\int_0^{\pi} d\theta \sin\theta\,\delta(E((k^2+q^2-2kq\cos\theta)^{1/2})-E(k)) = \frac{|M|^2V}{2\pi\hbar^2 v_g(k)}\int_0^{2k} dq\, q=\frac{|M|^2Vk^2}{\pi\hbar^2 v_g(k)} , \tag{4.1}$$

where V is the quantization volume and $v_g(k)$ is the group velocity of the excitonic polariton with wave vector k. As seen from this expression, $\Gamma_{\mathrm{imp}}(k)$ shows an increase in the exciton resonance region due to the decrease of the group velocity and the increase of the wave vector k. The energy dependence of $\Gamma_{\mathrm{imp}}(k)$ is similar to the experimental result. On the other hand, the estimation of the absolute value of $\Gamma_{\mathrm{imp}}(k)$ cannot be precise since the magnitude of the matrix element M is uncertain. For a rough estimate, one may treat the scattering classically. The scattering cross section can be supposed to be the square of the exciton Bohr radius which is about 7 Å in CuCl.[20] The group velocity of the excitonic polariton in the off-resonance region is of the order of one hundredth of the light velocity in a vacuum. If the impurity concentration N_i is assumed to be 10^{14} cm^{-3}, one can estimate the order of Γ_{imp} as

$$\Gamma_{\mathrm{imp}} \cong (7\ \text{Å})^2 v_g N_i = 1.5\times 10^8\ \mathrm{s}^{-1} . \tag{4.2}$$

This value is smaller by a few orders of magnitude than the experimentally estimated value. However, it is premature to rule out the impurity scattering as a mechanism of the dephasing relaxation of the excitonic polariton. To clarify the role of impurity scattering quantitatively, it is necessary to study the sample dependence of the dephasing relaxation constant by varying the impurity concentration systematically.

To examine the second possibility, the scattering probability is calculated for both the deformation potential coupling with longitudinal acoustic (ac) phonons and the Fröhlich interaction with longitudinal optic (op) phonons. The LA-phonon scattering rate via the deformation-potential coupling is given by

$$\Gamma_{\rm ac}(k)=\frac{2\pi}{\hbar}\sum_q |V_{\rm ac}(q)|^2[n_q\delta(E(k)-E(k+q)+\hbar\omega_q)+(1+n_q)\delta(E(k)-E(k-q)-\hbar\omega_q)]\ , \tag{4.3}$$

where the first term in the square brackets represents the contribution from the phonon absorption process and the second term that from the phonon emission process. $E(k)$ denotes the energy dispersion of the excitonic polariton and $\hbar\omega_q$ the acoustic phonon energy at wave vector q. For the case of a $1s$ exciton, the exciton-phonon coupling constant $V_{\rm ac}(q)$ is given by[21]

$$V_{\rm ac}(q)=\left[\frac{\hbar q}{2\rho u V}\right]^{1/2}[D_c f_c(q)-D_v f_v(q)]\ , \tag{4.4}$$

with

$$f_c(q)=1/[1+(\alpha_h a_B q/2)^2]^2$$

and (4.5)

$$f_v(q)=1/[1+(\alpha_e a_B q/2)^2]^2\ ,$$

where ρ, u, V, a_B, and D_c (D_v) denote the mass density, the sound velocity of LA phonons, the quantization volume, the exciton Bohr radius, and the deformation potential constant for the conduction (valence) band, respectively, and α_h and α_e are defined by

$$\alpha_h=m_h/(m_h+m_e),\quad \alpha_e=m_e/(m_h+m_e) \tag{4.6}$$

with the electron (hole) effective mass m_e (m_h). The coupling constant (4.4) is usually approximated in the small momentum limit as

$$V_{\rm ac}(q)\cong\left[\frac{\hbar q}{2\rho u V}\right]^{1/2}(D_c-D_v)\ . \tag{4.7}$$

Strictly speaking, (4.3) should be multiplied by another factor relating to the exciton content in the polariton mode. However, the exciton content is a slowly varying function with respect to the polariton energy and is almost unity over a rather wide range of 50—60 meV around the exciton resonance in the case of CuCl. Thus, the factor of the exciton content in the polariton mode can be safely neglected. In the calculation the following parameters are employed: $u=3.8\times10^5$ cm/s,[22] $\rho=4.16$ g/cm^3,[23] $D_c-D_v=-0.4$ eV,[24] and the temperature is taken to be 2 K. The calculated result is shown in Fig. 7. In the energy region above ω_l the results are shown for both the upper- and lower-branch polaritons. The increasing trend of the LA-phonon scattering rate as the energy approaches the exciton resonance is in agreement with the experimental result in Fig. 6. However, the absolute value of the scattering rate is much smaller than the experimental value. Thus, it can be concluded that LA-phonon scattering is only a minor mechanism of the dephasing relaxation of the excitonic polariton.

Similarly the LO-phonon scattering rate can be calculated. In this case the exciton-phonon coupling is induced through the Fröhlich interaction and its explicit form is given by[21]

$$V_{\rm op}(q)=\left[\frac{2\pi e^2\hbar\omega_{\rm LO}}{V}\left(\frac{1}{\epsilon_\infty}-\frac{1}{\epsilon_0}\right)\right]^{1/2}[f_c(q)-f_v(q)]/q\ , \tag{4.8}$$

where $\epsilon_\infty(\epsilon_0)$ and $\hbar\omega_{\rm LO}$ are the optic (static) dielectric constant and the LO-phonon energy, respectively, and f_c and f_v are defined in (4.5). Taking into account only the phonon-emission process, one obtains the following scattering rate due to the LO phonon:

$$\Gamma_{\rm op}(k)=\frac{2\pi}{\hbar}\sum_q |V_{\rm op}(q)|^2\delta(E(k)-E(k-q)-\hbar\omega_q)\ . \tag{4.9}$$

The relevant parameters are chosen as $\hbar\omega_{\rm LO}=26$ meV,[25] $\epsilon_\infty=5.0$,[13] $\epsilon_0=\epsilon_\infty\omega_l^2/\omega_t^2$, $\hbar\omega_l=3.2080$ eV,[13] and $\hbar\omega_t=3.2025$ eV.[13] The calculated result is shown in Fig. 8. The general trend of the energy dependence is similar to that in Fig. 7. In this case also, the absolute value of Γ is too small to explain the experimental results. On the basis of these results one can conclude that phonon

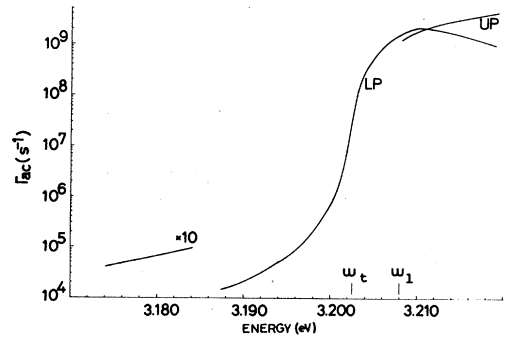

FIG. 7. Dephasing (momentum) relaxation rate of the excitonic polariton in CuCl due to the acoustic phonon scattering. Above the longitudinal exciton energy ω_l the results are shown for both the upper- (UP) and lower- (LP) branch polaritons.

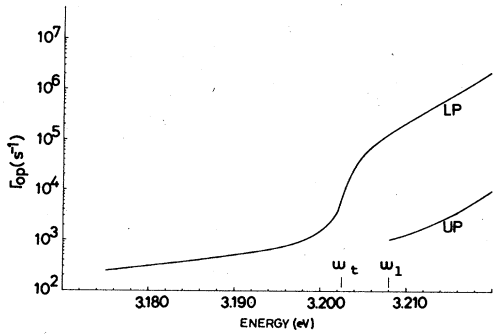

FIG. 8. Dephasing (momentum) relaxation rate of the excitonic polariton in CuCl due to the optic phonon scattering. Above the longitudinal exciton energy ω_l the results are shown for both the UP and LP branch polaritons.

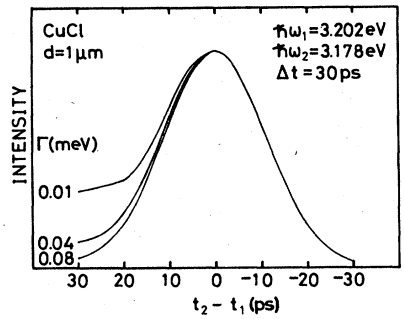

FIG. 9. Correlation traces of nondegenerate four-wave mixing for a 1-μm-thick CuCl crystal. The pulse width Δt (FWHM) is chosen to be 30 ps and the dephasing relaxation constant Γ is varied at 0.01, 0.04, and 0.08 meV (see text in Sec. VI).

scattering makes a minor contribution to the momentum relaxation of the excitonic polariton and cannot explain quantitatively the experimental results.

Let us finally examine the possibility of polariton-polariton scattering. Even when a well-collimated laser beam is concerned, there is uncertainty with respect to the direction of the polariton wave vector of the order of 0.1°. This broadening of the polariton wave vector may lead to mutual collisions among polaritons injected by an intense laser beam. The two colliding excitonic polaritons can scatter into various directions of the wave vector conserving the total energy and momentum. When the propagation direction of the scattered polariton is appreciably deflected from that of the incident polaritons, the scattered polariton cannot contribute to the signal intensity of the four-wave mixing. Even if the scattered polariton propagates in almost the same direction as the incident polaritons, the energy of the scattered polariton is not necessarily equal to that of the incident polariton. When detection is spatially well collimated and is also energetically well resolved, almost none of the scattered polaritons can contribute to the signal intensity. Thus, polariton-polariton scattering leads to the dephasing or momentum relaxation of the excitonic polariton. When the polariton-polariton scattering matrix element is written as

$$W(k_1,k_2;k_3,k_4)\ C^{\dagger}_{k_1}C^{\dagger}_{k_2}C_{k_3}C_{k_4}\ , \tag{4.10}$$

denoting the creation (annihilation) operator of the excitonic polariton with wave vector k by $C^{\dagger}_{k}$ (C_k), the momentum relaxation rate of an excitonic polariton with wave vector k is given by

$$\Gamma_c(k)=\frac{2\pi}{\hbar}\sum_{k_1,k_2,k_3}|W(k_1,k_2;k_3,k)|^2(1+N_{k_1})(1+N_{k_2})N_{k_3}\delta(k_1+k_2-k_3-k)\delta(E(k_1)+E(k_2)-E(k_3)-E(k))\ , \tag{4.11}$$

where $N(k)$ is the occupation number of the excitonic polariton with wave vector k. In (4.11) N_{k_1} and N_{k_2} can be neglected since the wave vector and energy of the scattered polaritons are in general different from those of the incident polaritons. The summation with respect to k_3 is carried out over the distribution of the incident polaritons. As a result, Γ_c is proportional to the laser intensity. Expression (4.11) can be reduced to a more convenient form for numerical calculation. Taking the z axis in the direction of wave vector $k+k_3$ and neglecting the wave-vector dependence of W, one can reduce (4.11) to

$$\begin{aligned}\Gamma_c(k)&=\frac{2\pi}{\hbar}|W|^2\sum_{k_3}N_{k_3}\sum_{k_1}\delta(E(k_1)+E(k+k_3-k_1)-E(k_3)-E(k))\\&=\frac{V}{2\pi\hbar^2}|W|^2\sum_{k_3}N_{k_3}\int_0^{\infty}d|k_1||k_1|^2\int_0^{\pi}d\theta\sin\theta\sum_{\alpha}\frac{\delta(|k_1|-|k_1^{\alpha}|)}{|f(\theta,|k_1^{\alpha}|)|}\ ,\end{aligned} \tag{4.12}$$

with

$$f(\theta,|k_1|)=v_g(|k_1|)+v_g(|k+k_3-k_1|)(|k_1|-|k+k_3|\cos\theta)/|k+k_3-k_1|\ , \tag{4.13}$$

where v_g is the group velocity of the excitonic polariton, V the quantization volume, and the superscript α indicates a number of solutions which satisfy the energy conservation implied by the δ function. It is found numerically that the integral in (4.12) is not sensitive to the angle between k and k_3 within a few degrees. Thus, it is permissible to replace the summation over k_3 in (4.12) by the value for a typical k_3 multiplied by the total number of incident polaritons. In the numerical estimate of the absolute value of Γ_c, the two colliding polaritons are assumed to have the same energy 3.188 eV ($|k|=|k_3|$) and the angle between the two wave vectors is chosen typically as 0.1°. Using the recent results of the microscopic calculation of the collision matrix element of excitonic polaritons in CuCl,[26] one finds a typical value

$$WV=4.8\times10^{-32}\ \text{erg}\ , \tag{4.14}$$

and obtains

$$\Gamma_c^{\text{theor}}(3.188\ \text{eV})=3.6\times10^{10}\ \text{s}^{-1}\ , \tag{4.15}$$

where the number density of the incident polaritons is

supposed to be 10^{18} cm^{-3}, estimated from the power, pulse width, beam diameter of the laser, and the crystal thickness. This value can be compared with the experimental result:

$$\Gamma_c^{\text{expt}}(3.188\ \text{eV})=1.5\times10^{10}\ \text{s}^{-1}\ . \tag{4.16}$$

These two values agree well within a factor 3. However, this agreement should be considered as fortuitous since there remains uncertainty in the estimation of the number density of polaritons and other dynamical parameters. In the theoretical fitting the absolute value of Γ is adjusted to the experimental value at 3.188 eV and the energy dependence of Γ is determined by (4.12). The calculated result is shown by a dashed line in Fig. 6. As for the energy dependence of Γ, the agreement between theory and experiment is satisfactory, although the experimental values are ambiguous in the resonance region.

From the above arguments it may be concluded that the dephasing or momentum relaxation of the excitonic polariton is caused mainly by polariton-polariton scattering under our experimental conditions, although impurity scattering cannot be ruled out as a mechanism of the dephasing relaxation.

V. MICROSCOPIC DERIVATION OF EQUATIONS OF MOTION AND DEPHASING RELAXATION OF EXCITONIC POLARITONS

In Sec. II, the basic equations of motion for the excitonic polariton are taken from the familiar ones in laser theory which are derived on the picture of localized excitations. However, the excitonic polariton is not a localized excitation but propagates throughout the crystal with a definite wave vector. In this section the basic equations of motion are derived from the microscopic point of view and it is confirmed that the same equations of motion as in laser theory are applicable for the case of excitonic polaritons with a small change to incorporate spatial dispersion. First of all let us derive the polarization field operator quantum mechanically from the electromagnetic interaction

$$\frac{e}{2mc}(\mathbf{p}\cdot\mathbf{A}+\mathbf{A}\cdot\mathbf{p})\ , \tag{5.1}$$

where $\mathbf{A}$ is the vector potential and $\mathbf{p}$ the momentum operator. In the second-quantized form the vector potential is written as

$$\mathbf{A}(r)=\sum_{q,\lambda}\left[\frac{2\pi\hbar c}{|q|V}\right]^{1/2}\hat{\mathbf{e}}_{q\lambda}e^{iqr}(b_{q\lambda}+b^{\dagger}_{-q\lambda})\ , \tag{5.2}$$

where b_q ($b_q^{\dagger}$), $\hat{\mathbf{e}}_{q\lambda}$ and V are the annihilation (creation) operator of the photon with wave vector q, the polarization vector, and the quantization volume, respectively, and the polarization index λ indicates the transverse modes in the Coulomb gauge. Calculating the matrix element between the electron field operators, one obtains

$$\int d^3r\,\Psi^{\dagger}(r)\frac{e}{2mc}(\mathbf{p}\cdot\mathbf{A}+\mathbf{A}\cdot\mathbf{p})\Psi(r)=\frac{ie}{mc}\left[\frac{2\pi\hbar c}{V}\right]^{1/2}\sum_{k,q,\lambda}\frac{\mathbf{p}_0\cdot\hat{\mathbf{e}}_{q\lambda}}{|q|^{1/2}}(a^{\dagger}_{c,k+q}a_{vk}-a^{\dagger}_{v,k+q}a_{ck})(b_{q\lambda}+b^{\dagger}_{-q\lambda})\ , \tag{5.3}$$

where $a^{\dagger}_{\alpha k}$ ($a_{\alpha k}$) is the creation (annihilation) operator of the α-band electron with wave vector k. The real vector $\mathbf{p}_0$ is defined by

$$i\,\mathbf{p}_0=\frac{1}{v_0}\int_{v_0}d^3r\,u^{*}_{ck'}(r)\mathbf{p}u_{vk}(r)\ , \tag{5.4}$$

where $u_{\alpha k}(r)$ denotes the periodic part of the Bloch function of the α band, v_0 the volume of the unit cell, and the usual s-p band combination is tacitly assumed for the conduction and valence bands. Here the wave-vector dependence of the matrix element is neglected. In the resonant-term approximation, (5.3) becomes

$$\frac{ie}{mc}\left[\frac{2\pi\hbar c}{V}\right]^{1/2}\sum_{k,q,\lambda}\frac{\mathbf{p}_0\cdot\hat{\mathbf{e}}_{q\lambda}}{|q|^{1/2}}\times(a^{\dagger}_{c,k+q}a_{vk}b_{q\lambda}-a^{\dagger}_{v,k+q}a_{ck}b^{\dagger}_{-q\lambda})\ . \tag{5.5}$$

On the other hand, the electric field is given by

$$\begin{aligned}\mathbf{E}(r)&=-\frac{1}{c}\frac{\partial}{\partial t}\mathbf{A}(r)\\&=\sum_{q,\lambda}i\left[\frac{2\pi\hbar c|q|}{V}\right]^{1/2}\hat{\mathbf{e}}_{q\lambda}e^{iqr}(b_{q\lambda}-b^{\dagger}_{-q\lambda})\\&=\sum_q e^{iqr}[\mathbf{E}^{-}(q)+\mathbf{E}^{+}(q)]=\sum_q e^{iqr}\mathbf{E}(q)\ ,\end{aligned} \tag{5.6}$$

where the Fourier component of the electric field $\mathbf{E}(q)$ is decomposed into the positive and negative frequency parts corresponding to $b^{\dagger}_{-q}$ and b_q, respectively. With these notations (5.5) is written as

$$\frac{e\,\mathbf{p}_0}{mc}\sum_{k,q}\frac{1}{|q|}[a^{\dagger}_{c,k+q}a_{vk}\mathbf{E}^{-}(q)+a^{\dagger}_{v,k+q}a_{ck}\mathbf{E}^{+}(q)]\ . \tag{5.7}$$

Supplementing the nonresonant terms, one obtains the second-quantized form of the electromagnetic interaction as

$$\frac{e}{mc}\sum_{k,q}\frac{p_0\cdot\mathbf{E}(q)}{|q|}(a^{\dagger}_{c,k+q}a_{vk}+a^{\dagger}_{v,k+q}a_{ck})\ . \tag{5.8}$$

From the analogy to the electromagnetic interaction in the dipole approximation, the polarization field operator with wave vector q can be introduced by

$$\mathbf{p}(q)=-\frac{e\mathbf{p}_0}{mc\,|\,q\,|}\sum_k(a^\dagger_{c,k+q}a_{vk}+a^\dagger_{v,k+q}a_{ck})\ . \tag{5.9}$$

The prefactor of (5.9), having the dimensions of the electric dipole moment, will be denoted by μ:

$$\mu=\frac{e\,|\,\mathbf{p}_0\,|}{mc\,|\,q\,|}\ , \tag{5.10}$$

where the typical value of q is determined by the exciton energy ϵ_x as

$$\hbar c\,|\,q\,|=\epsilon_x\ . \tag{5.11}$$

On the other hand, the quantity corresponding to the population inversion is defined by

$$I(r)=(a^\dagger_{cr}a_{cr}-a^\dagger_{vr}a_{vr})/v_0\ , \tag{5.12}$$

where $a^\dagger_{\alpha r}$ ($a_{\alpha r}$) is the creation (annihilation) operator of the α-band electron in the Wannier representation and v_0 is the volume of the unit cell. The Fourier component of the population inversion, defined by

$$\sigma(q)=\int d^3r e^{iqr}I(r)\ , \tag{5.13}$$

can be written as

$$\sigma(q)=\sum_k(a^\dagger_{c,k+q}a_{ck}-a^\dagger_{v,k+q}a_{vk}) \tag{5.14}$$

by transforming the Wannier operators into the Bloch operators.

Now that the operators of the polarization field and of the population inversion are derived microscopically, the equations of motion for these variables will be considered. The Hamiltonian is assumed in the simplest form as

$$H=\sum_k E_c(k)a^\dagger_{ck}a_{ck}+\sum_k E_v(k)a^\dagger_{vk}a_{vk}+i\sum_{k,q,\lambda}g_\lambda(q)(a^\dagger_{c,k+q}a_{vk}b_{q\lambda}-a^\dagger_{vk}a_{c,k+q}b^\dagger_{q\lambda})\ , \tag{5.15}$$

where $E_\alpha(k)$ is the energy dispersion of the α-band electron and the electromagnetic coupling constant is defined by

$$g_\lambda(q)=\frac{e\mathbf{p}_0\cdot\hat{\mathbf{e}}_{q\lambda}}{mc}\left[\frac{2\pi\hbar c}{V\,|\,q\,|}\right]^{1/2}\ . \tag{5.16}$$

A typical equation of motion is given as

$$\frac{d}{dt}a^\dagger_{c,k+q}a_{vk}=\frac{i}{\hbar}[H,a^\dagger_{c,k+q}a_{vk}]=\frac{i}{\hbar}[E_c(k+q)-E_v(k)]a^\dagger_{c,k+q}a_{vk}-\frac{ie\,|\,\mathbf{p}_0\,|}{\hbar mc}\sum_{q'}(a^\dagger_{c,k+q}a_{c,k-q'}-a^\dagger_{v,k+q+q'}a_{vk})E^+(q')/|\,q'\,|\ , \tag{5.17}$$

where $E^+(q)$ is the positive frequency part of the electric field defined in (5.6). Hereafter, the electric field component parallel to $\mathbf{p}_0$ will be considered. Taking the sum over wave vector k on both sides of (5.17), replacing $|\,q'\,|$ in the denominator on the right-hand side by a typical value given in (5.11), and introducing the replacement

$$E_c(k+q)-E_v(k)\cong\epsilon_x(q) \tag{5.18}$$

with the exciton energy dispersion $\epsilon_x(q)$, one finds

$$\frac{d}{dt}\sum_k a^\dagger_{c,k+q}a_{vk}=\frac{i}{\hbar}\epsilon_x(q)\sum_k a^\dagger_{c,k+q}a_{vk}-\frac{i}{\hbar}\mu\sum_{q'}\sigma(q+q')E(q')\ , \tag{5.19}$$

where the negative frequency part of the electric field is added to the second term on the right-hand side and the notation of (5.10) is used. In the same way one obtains

$$\frac{d}{dt}\sum_k a^\dagger_{v,k+q}a_{ck}=-\frac{i}{\hbar}\epsilon_x(q)\sum_k a^\dagger_{v,k+q}a_{ck}+\frac{i}{\hbar}\mu\sum_{q'}\sigma(q+q')E(q')\ . \tag{5.20}$$

The basic equations of motion for the polarization field operator are derived by adding (5.19) and (5.20) or by subtracting (5.20) from (5.19) as

$$\frac{d}{dt}p(q)=-\frac{i\mu}{\hbar}\epsilon_x(q)\sum_k(a^\dagger_{c,k+q}a_{vk}-a^\dagger_{v,k+q}a_{ck})\ , \tag{5.21}$$

$$\frac{d}{dt}\mu\sum_k(a^\dagger_{c,k+q}a_{vk}-a^\dagger_{v,k+q}a_{ck})=-\frac{i}{\hbar}\epsilon_x(q)p(q)-\frac{2i\mu^2}{\hbar}\sum_{q'}\sigma(q+q')E(q')\ , \tag{5.22}$$

where $p(q)$ is the magnitude of the vector in (5.9).

Next, the equation of motion for the population inversion is derived:

$$\frac{d}{dt}a^\dagger_{c,k+q}a_{ck}=\frac{i}{\hbar}[E_c(k+q)-E_c(k)]a^\dagger_{c,k+q}a_{ck}+\frac{ie\,|\,\mathbf{p}_0\,|}{\hbar mc}\sum_{q'}\frac{1}{|\,q'\,|}[a^\dagger_{v,k+q+q'}a_{ck}E^+(q')-a^\dagger_{c,k+q}a_{v,k-q'}E^-(q')]\ , \tag{5.23}$$

$$\frac{d}{dt}a^\dagger_{v,k+q}a_{vk}=\frac{i}{\hbar}[E_v(k+q)-E_v(k)]a^\dagger_{v,k+q}a_{vk}+\frac{ie\,|\,\mathbf{p}_0\,|}{\hbar mc}\sum_{q'}\frac{1}{|\,q'\,|}[a^\dagger_{c,k+q+q'}a_{vk}E^-(q')-a^\dagger_{v,k+q}a_{c,k-q'}E^+(q')]\ . \tag{5.24}$$

The first term on the right-hand side of each equation represents wavelike behavior due to the dispersion of the energy band. Since q denotes the wave vector of the population grating and is usually small, the first terms on the right-hand side can be safely neglected. By repeating the same procedure as in the derivation of (5.19) from (5.17), one obtains

$$\frac{d}{dt}\sigma(q)=-\frac{2i\mu}{\hbar}\sum_{q'}E(q')\sum_{k}(a^{\dagger}_{c,k+q+q'}a_{vk}-a^{\dagger}_{v,k+q+q'}a_{ck}) . \tag{5.25}$$

Equations (5.21), (5.22), and (5.25) form the basis set for the dynamical description of the excitonic polariton. Let us now introduce the real-space field operators defined by

$$\begin{aligned} &I(r)=\frac{1}{V}\sum_{q}e^{-iqr}\sigma(q),\quad p(r)=\frac{1}{V}\sum_{q}e^{-iqr}p(q) ,\\ &p^{+}(r)=\frac{-\mu}{V}\sum_{k,q}e^{-iqr}a^{\dagger}_{c,k+q}a_{vk} ,\\ &p^{-}(r)=\frac{-\mu}{V}\sum_{k,q}e^{-iqr}a^{\dagger}_{v,k+q}a_{ck} , \end{aligned} \tag{5.26}$$

where, of course, it holds that $p(r)=p^{+}(r)+p^{-}(r)$. Then the equations of motion for these operators are obtained as

$$\frac{d}{dt}p(r)=\frac{i}{\hbar}\epsilon_x(i\nabla)[p^{+}(r)-p^{-}(r)] , \tag{5.27}$$

$$\frac{d}{dt}[p^{+}(r)-p^{-}(r)]=\frac{i}{\hbar}\epsilon_x(i\nabla)p(r)+\frac{2i\mu^2}{\hbar}I(r)E(r) , \tag{5.28}$$

$$\frac{d}{dt}I(r)=\frac{2i}{\hbar}E(r)[p^{+}(r)-p^{-}(r)] . \tag{5.29}$$

Here the field quantities are scalars since, as mentioned before, the electric field component parallel to the polarization field is considered.

It is quite instructive to compare these equations with the density-matrix equations for a two-level atom. The latter are familiar in laser theory[7,8] and are given explicitly as

$$\frac{d}{dt}\rho_{12}=i\omega_0\rho_{12}+\frac{i\mu}{\hbar}E\sigma-\gamma_{\perp}\rho_{12} , \tag{5.30}$$

$$\frac{d}{dt}\sigma=\frac{i2\mu}{\hbar}E(\rho_{12}-\rho^{*}_{12})+\gamma_{\parallel}(\sigma_0-\sigma) . \tag{5.31}$$

Here the upper (lower) level of a two-level atom is denoted by 2 (1) and σ, σ_0, $\hbar\omega_0$, μ, and $\gamma_{\parallel}$ ($\gamma_{\perp}$) are the population inversion defined by $\rho_{22}-\rho_{11}$, the equilibrium value of σ, the energy difference between the two levels, the electric dipole moment, and the longitudinal (transverse) relaxation constant, respectively. The polarization defined by

$$p=\mu(\rho_{12}+\rho^{*}_{12}) , \tag{5.32}$$

satisfies the equation

$$\frac{d}{dt}p=-\gamma_{\perp}p+i\omega_0\mu(\rho_{12}-\rho^{*}_{12}) . \tag{5.33}$$

Another relevant equation is derived from (5.30) and is given by

$$\frac{d}{dt}\mu(\rho_{12}-\rho^{*}_{12})=i\omega_0 p+\frac{2i\mu^2}{\hbar}E\sigma-\gamma_{\perp}\mu(\rho_{12}-\rho^{*}_{12}) . \tag{5.34}$$

It is easily seen that the equations of motion from (5.27) to (5.29) have a one-to-one correspondence with the set of equations (5.33), (5.34), and (5.31), if the relaxation terms in the latter are dropped and the following correspondence is supposed:

$$\mu\rho_{12}\leftrightarrow p^{+}(r),\quad \mu\rho^{*}_{12}\leftrightarrow p^{-}(r) . \tag{5.35}$$

Thus, the equations of motion, which were originally derived in laser theory, turn out to be applicable in the case of excitonic polaritons with a small change to incorporate spatial dispersion. In fact Eqs. (2.1) and (2.2) can be derived from (5.27) and (5.29) with the replacement of $2\omega_t\mu^2/\hbar$ by $\beta\omega_t^2$.

Next, the inclusion of the relaxation terms will be discussed from the microscopic point of view.[27] The relaxation phenomena result from the reversible dynamical equations of motion, when some kind of coarse graining is introduced which is closely related to the method of measurements; for example, the phonon state of the crystal lattice is not measured and the signal emitted in a particular direction is selectively observed. The procedure of coarse graining can be incorporated by means of the general method of projection[28,29] to derive the irreversibility from reversible dynamics. In the following let us derive the relaxation terms due to the polariton-phonon interaction and the polariton-polariton scattering. In the procedure of coarse graining the total system is divided into the relevant system and the rest, which is usually called the reservoir, and the dynamics of the total system are projected onto that of the relevant system by eliminating the degrees of freedom of the reservoir. To be more concrete, let us consider the reduced density operator defined by

$$\rho_r=P\rho , \tag{5.36}$$

where P is a suitable projection operator. The equation of motion for ρ_r is generally given by[30]

$$\begin{aligned} \frac{d}{dt}\rho_r(t)=&-\frac{i}{\hbar}L_S\rho_r(t)\\ &-\frac{1}{\hbar^2}\int_0^t d\tau PL_{SR}e^{-i(1-P)L(t-\tau)/\hbar}L_{SR}\rho_r(\tau) , \end{aligned} \tag{5.37}$$

where the Hamiltonian of the total system is divided into those of the relevant system (S), the reservoir (R) and their interaction (SR) as

$$H=H_S+H_R+H_{SR} , \tag{5.38}$$

and the Liouville operators are defined, for any operator A, by

$$LA=[H,A],\quad L_SA=[H_S,A],\quad L_{SR}A=[H_{SR},A] . \tag{5.39}$$

In the case of the polariton-phonon interaction, the relevant system and the reservoir correspond to the exci-

tonic polaritons and the phonon system, respectively. The suitable projection operator is given by

$$P\rho=\rho_{\rm ph}^{0}{\rm Tr}_{\rm ph}\rho=\rho_{\rm ph}^{0}\rho_S\ , \tag{5.40}$$

where $\rho_{\rm ph}^{0}$ denotes the thermal equilibrium state of the phonon system, the trace is over the phonon states, and ρ_S is the density operator only for the excitonic polaritons. It is convenient to use the polariton operator instead of the electron-hole excitation operator. Let $C_{\lambda k}^{\dagger}$ ($C_{\lambda k}$) denote the creation (annihilation) operator of the excitonic polariton with wave vector k, where the index λ specifies the electron-hole relative motion. The polariton-phonon interaction Hamiltonian can be written as

$$H_{\rm ep}=\sum_{k,q}\Xi(q)C_{k+q}^{\dagger}C_k(b_q+b_{-q}^{\dagger})\ , \tag{5.41}$$

where $b^{\dagger}$ (b) is the creation (annihilation) operator of phonons and $\Xi(q)$ is the coupling strength dependent on the kind of phonons and on the exciton internal motion. Here the electron-hole relative motion is assumed to be the lowest $1s$ state and the index λ is dropped. Then by substitution of $H_{\rm ep}$ for H_{SR}, the second term of (5.37) can be calculated up to the second-order perturbation with respect to $H_{\rm SR}$ as

$$-\frac{1}{\hbar^2}\sum_{k,k',q}|\Xi(q)|^2\int_0^t d\tau\{[n_q e^{-i\omega_q\sigma}+(1+n_q)e^{i\omega_q\sigma}][C_{k'-q}^{\dagger}C_{k'},C_{k+q}^{\dagger}(\sigma)C_k(\sigma)e^{iH_S\sigma/\hbar}\rho_S(\tau)e^{-iH_S\sigma/\hbar}]$$
$$+[n_q e^{i\omega_q\sigma}+(1+n_q)e^{-i\omega_q\sigma}][e^{iH_S\sigma/\hbar}\rho_S(\tau)e^{-iH_S\sigma/\hbar}C_{k+q}^{\dagger}(\sigma)C_k(\sigma),C_{k'-q}^{\dagger}C_{k'}]\}\ , \tag{5.42}$$

where $\sigma=\tau-t$ and ω_q and n_q denote the frequency and the occupation number of the phonon with wave vector q, respectively. The Heisenberg operator is defined in terms of H_S in (5.38), namely, the Hamiltonian of the excitonic polariton. Taking into account only the secular terms and employing the Markovian approximation,[30] one can further reduce (5.42) to

$$-\frac{2\pi}{\hbar}\sum_{k,q}|\Xi(q)|^2\{[n_q\delta(E(k+q)-E(k)-\hbar\omega_q)+(1+n_q)\delta(E(k+q)-E(k)+\hbar\omega_q)][C_k^{\dagger}C_{k+q},C_{k+q}^{\dagger}C_k\rho_S(t)]$$
$$+[n_q\delta(E(k+q)-E(k)+\hbar\omega_q)+(1+n_q)\delta(E(k+q)-E(k)-\hbar\omega_q)][\rho_S(t)C_{k+q}^{\dagger}C_k,C_k^{\dagger}C_{k+q}]\}=\Gamma_{\rm ph}\rho\ , \tag{5.43}$$

where the polariton dispersion is denoted by $E(k)$ and the relaxation operator $\Gamma_{\rm ph}$ is defined by this equation. Consequently, the equation of motion for the reduced density operator ρ_S in (5.40) becomes

$$\frac{d}{dt}\rho_S(t)=-\frac{i}{\hbar}[H_S,\rho_S]+\Gamma_{\rm ph}\rho_S\ . \tag{5.44}$$

In order to derive the equations of motion for physical quantities, the average value of some operator A, defined by

$$\langle A(t)\rangle={\rm Tr}A\rho_S(t)\ , \tag{5.45}$$

will be considered. The equation of motion for the averaged quantity $\langle A(t)\rangle$ is given as

$$\frac{d}{dt}\langle A(t)\rangle={\rm Tr}A\frac{d}{dt}\rho_S(t)=\frac{i}{\hbar}{\rm Tr}\rho_S[H_S,A]+{\rm Tr}A\Gamma_{\rm ph}\rho_S\ . \tag{5.46}$$

The Fourier component of the polarization field with wave vector Q can be written in terms of the polariton operator as

$$p(Q)=-\mu(C_Q^{\dagger}+C_{-Q})\ . \tag{5.47}$$

The damping of the polarization field component $p(Q)$ arising from the second term of (5.46) is calculated as

$$\frac{2\pi}{\hbar}\sum_q|\Xi(q)|^2\{[n_q\delta(E(Q)-E(Q-q)-\hbar\omega_q)+(1+n_q)\delta(E(Q)-E(Q-q)+\hbar\omega_q)]\langle C_{Q-q}^{\dagger}C_{Q-q}\rangle$$
$$-[n_q\delta(E(Q)-E(Q-q)+\hbar\omega_q)+(1+n_q)\delta(E(Q)-E(Q-q)-\hbar\omega_q)]\langle C_{Q-q}C_{Q-q}^{\dagger}\rangle\}p(Q)\ , \tag{5.48}$$

where a decoupling approximation such as

$${\rm Tr}C_K^{\dagger}C_KC_Q\rho_S(t)\cong\langle C_Q\rangle\langle C_K^{\dagger}C_K\rangle\ , \tag{5.49}$$

is employed. When $\langle C_k^{\dagger}C_k\rangle$ is regarded as the population of polaritons with wave vector k, the first term of (5.48) can be interpreted as the rate coming into the polariton state with wave vector Q, whereas the second term can be interpreted as the rate leaving the same polariton state. If only the polariton state with wave vector Q is occupied in the initial state, only the second term of (5.48) does not vanish and gives exactly the same damping constant as in (4.3).

Now let us consider the relaxation term due to polariton-polariton scattering. In this case the relevant system is the ensemble of polaritons with a particular range of wave vectors contained in the incident beam; the reservoir corresponds to the other polaritons, which will be referred to as the reservoir polaritons. The suitable projection operator is given by

$$P\rho = |0'\rangle\langle 0'|\,\mathrm{Tr}'\rho\ , \tag{5.50}$$

where $|0'\rangle$ denotes the vacuum state with respect to the reservoir polaritons and the primed trace implies the trace operation over the reservoir polaritons. The polariton-polariton scattering Hamiltonian is given by (4.10). Then by a similar calculation as in (5.42), the relaxation operator in the Markovian approximation is derived:

$$\Gamma_c\rho = -\frac{2\pi}{\hbar}\sum_{k_1,k_2}\sum_{k_3,k_4}{}'\,\delta(E(k_1)+E(k_2)-E(k_3)-E(k_4))\,|W(k_1,k_2;k_3,k_4)|^2\{[C^\dagger_{k_1}C^\dagger_{k_2},C_{k_1}C_{k_2}\rho]+[\rho C^\dagger_{k_1}C^\dagger_{k_2},C_{k_1}C_{k_2}]\}\ , \tag{5.51}$$

where the summation with respect to k_1 and k_2 is over the relevant polaritons, whereas the sum concerning k_3 and k_4 is over the reservoir polaritons and is indicated by a prime. The damping constant of the polarization field component $p(Q)$ due to the relaxation operator Γ_c is calculated from (5.46) and (5.51) as

$$-\frac{2\pi}{\hbar}\sum_{k_1}\sum_{k_3,k_4}{}'\,|W(k_1,Q;k_3,k_4)|^2 N_{k_1}\times\delta(E(k_1)+E(Q)-E(k_3)-E(k_4))\langle p(Q)\rangle\ , \tag{5.52}$$

where the decoupling approximation as in (5.49) is employed and N_k represents $\langle C^\dagger_k C_k\rangle$. This expression is exactly in agreement with (4.11) as it should be.

In summary, the basic equations of motion for the excitonic polariton are derived microscopically and given a firm basis. It is confirmed that the equations of motion familiar in laser theory are applicable also in the case of excitonic polaritons with the inclusion of spatial dispersion. At the same time, the damping of the polarization field that is identified with the dephasing relaxation of the excitonic polariton is derived by the standard statistical mechanical method using projection operators and it is confirmed that up to second-order perturbation the statistical mechanical method gives the same result as the golden-rule calculation.

VI. SUMMARY AND DISCUSSION

The concept of the dephasing relaxation of the excitonic polariton has been clarified for the first time and the method of analysis of the experimental data of nondegenerate four-wave mixing has been established. The various mechanisms of the dephasing relaxation of the excitonic polariton are discussed and the most probable mechanism is identified as the polariton-polariton collision. The observed dephasing relaxation constant of the excitonic polariton in CuCl is of the order of 0.01 meV and increases as the energy approaches the exciton resonance.

The conceptual difference between the dephasing relaxation of the localized excitation and of the propagating elementary excitation has to be emphasized. In the former the dephasing relaxation or, in other words, the transverse relaxation is related to the decay of the coherence of the relevant transition or of the off-diagonal component of the density matrix. In the latter case, however, the excitations are not localized but propagate throughout the crystal with a definite wave vector. Accordingly, the coherence of the relevant transition, which is usually related to the polarization field, has the degree of freedom of the wave vector. This degree of freedom is one of the salient features of the propagating elementary excitation which make a striking contrast with the case of the localized excitation. In addition to the wave vector the excitonic polariton has a degree of freedom of the exciton internal state, i.e., the electron-hole relative motion. The change of the exciton internal state may lead to the fluctuation and relaxation of the exciton coherence, since the oscillator strength of the exciton depends on the exciton internal state. The dephasing relaxation due to the change of the exciton internal state may be caused by a mutual collision among the excitonic polaritons under a rather high excitation. In this paper, however, the dephasing relaxation due to a change of wave vector has been discussed exclusively.

In the exciton resonance region, as mentioned in Sec. III, the correlation trace becomes insensitive to the dephasing relaxation constant Γ and the experimental value of Γ cannot be determined precisely. Let us make a few proposals to overcome this difficulty. The simplest one in principle is the use of a pulse with width comparable to the dephasing relaxation time. In the limit of infinitesimal pulse width, as shown in Sec. II, the correlation trace shows directly the decay due to the imaginary part of the wave vector. Thus, an improvement in the precision of measuring Γ can be expected by use of shorter pulses. A second proposal is to use a thinner sample. Let us consider a thin sample whose thickness is of the same order as the absorption length of the excitonic polariton, namely, the inverse of the imaginary part of the wave vector. In this case the simple expression (3.13) cannot be used and one has to calculate the full expression (3.4). The correlation trace can be expected to be sensitive to the value of Γ. In fact, for a 1-μm-thick sample of CuCl one obtains correlation traces sensitive to the value of Γ, as shown in Fig. 9. Thus, the value of Γ can be fixed from curve fitting if the value lies within the range shown in the figure.

Finally let us point out a few interesting proposals for future study. The first one is the use of two-photon excitation of the upper-branch polariton. This excitation scheme was first devised by Fröhlich *et al.*[31,32] to measure the polariton dispersion in CuCl. By two-photon excitation an upper-branch polariton can be created almost uniformly in a sample because the fundamental photon energy lies in the transparent region of the crystal. Furthermore, this excitation scheme can create an upper-branch polariton selectively without excitation of the lower-branch polariton owing to wave-vector conservation. Thus, the troublesome additional boundary conditions (ABC) problem[33] can be avoided and the dephasing relaxation constant of the upper-branch polariton can be measured precisely, although the tunable energy range may be rather limited. A second proposal is the use of reflection-type four-wave mixing. As is well known, the pseudogap region is highly absorptive and shows a high reflectivity. Thus, it is desirable to measure the four-wave mixing signal in reflection geometry rather than in transmission geometry. In fact, four-wave mixing in reflection geometry is successfully observed in CuCl (Ref. 34) using nanosecond laser pulses. Since the excitonic polariton in the pseudogap region has a very short penetration depth in the crystal, one can probe the relaxation of the excitonic polariton in the vicinity of the crystal surface by means of reflection-type four-wave mixing.

ACKNOWLEDGMENTS

The author would like to thank Professor S. Shionoya and Dr. Y. Masumoto for close collaboration and enlightening discussions. Thanks are also due to Professor T. Yajima, Professor Y. Toyozawa, Professor E. Hanamura, Professor M. Matsuoka, and Professor N. Nagasawa for enlightening discussions and critical comments.

[1]Y. Masumoto, S. Shionoya, and T. Takagahara, Phys. Rev. Lett. **51**, 923 (1983).
[2]T. Yajima and H. Souma, Phys. Rev. A **17**, 309 (1978).
[3]T. Yajima, H. Souma, and Y. Ishida, Phys. Rev. A **17**, 324 (1978).
[4]A. Laubereau and W. Kaiser, Rev. Mod. Phys. **50**, 607 (1978).
[5]W. H. Hesselink and D. A. Wiersma, Phys. Rev. Lett. **43**, 1991 (1979).
[6]I. D. Abella, N. A. Kurnit, and S. R. Hartmann, Phys. Rev. **141**, 391 (1966).
[7]N. Bloembergen, *Nonlinear Optics* (Benjamin, New York, 1965).
[8]K. Shimoda, T. Yajima, Y. Ueda, T. Shimizu, and T. Kasuya, *Quantum Electronics* (Shokabo, Tokyo, 1970) (in Japanese).
[9]J. J. Hopfield and D. G. Thomas, Phys. Rev. **132**, 563 (1963).
[10]T. Mita, K. Sotome, and M. Ueta, Solid State Commun. **33**, 1135 (1980).
[11]T. Mita, K. Sotome, and M. Ueta, J. Phys. Soc. Jpn. **48**, 496 (1980).
[12]Y. Segawa, Y. Aoyagi, K. Azuma, and S. Namba, Solid State Commun. **28**, 853 (1978).
[13]Y. Masumoto, Y. Unuma, Y. Tanaka, and S. Shionoya, J. Phys. Soc. Jpn. **47**, 1844 (1979).
[14]N. Bloembergen and P. S. Pershan, Phys. Rev. **128**, 606 (1962).
[15]T. Mita and N. Nagasawa, Solid State Commun. **44**, 1003 (1982).
[16]T. Itoh and T. Suzuki, J. Phys. Soc. Jpn. **45**, 1939 (1978).
[17]R. Levy, B. Hönerlage, and J. B. Grun, Solid State Commun. **29**, 103 (1979).
[18]Y. Segawa, Y. Aoyagi, and S. Namba, Solid State Commun. **39**, 535 (1981).
[19]Y. Masumoto and S. Shionoya, J. Phys. Soc. Jpn. **51**, 181 (1982).
[20]E. Hanamura, in *Excitons at High Density,* edited by H. Haken and S. Nikitine (Springer, Berlin, 1975), p. 43.
[21]Y. Toyozawa, Prog. Theor. Phys. **20**, 53 (1958).
[22]R. C. Hanson, K. Helliwell, and C. Schwab, Phys. Rev. B **9**, 2649 (1974).
[23]T. H. K. Barron, J. A. Birch, and G. K. White, J. Phys. C **10**, 1617 (1977).
[24]J. B. Anthony, A. D. Brothers, and D. W. Lynch, Phys. Rev. B **5**, 3189 (1972).
[25]M. Kalm and Ch. Uihlein, Phys. Status Solidi B **87**, 575 (1978).
[26]T. Takagahara and J. L. Birman, Phys. Rev. B **28**, 6161 (1983).
[27]T. Takagahara, in *Semiconductors Probed by Ultrafast Laser Spectroscopy,* edited by R. R. Alfano (Academic, New York, 1984), p. 331.
[28]S. Nakajima, Prog. Theor. Phys. **20**, 948 (1958).
[29]R. Zwanzig, Phys. Rev. **124**, 983 (1961).
[30]T. Takagahara, E. Hanamura, and R. Kubo, J. Phys. Soc. Jpn. **44**, 728 (1978).
[31]D. Fröhlich, E. Mohler, and P. Wiesner, Phys. Rev. Lett. **26**, 554 (1971).
[32]D. Fröhlich, E. Mohler, and Ch. Uihlein, Phys. Status Solidi B **55**, 175 (1973).
[33]J. L. Birman, in *Excitons,* edited by E. I. Rashba and M. D. Sturge (North-Holland, Amsterdam, 1982), Chap. 2.
[34]G. Mizutani and N. Nagasawa, Opt. Commun. **50**, 31 (1984).